Journal of
Marine Science and Engineering

MDPI

Article

An Output Power Interval Control Strategy Based on Pseudo-Tip-Speed Ratio and Adaptive Genetic Algorithm for Variable-Pitch Tidal Stream Turbine

Youming Cai [1], Mingzhu Li [1], Tianzhen Wang [1,*], Xiaohang Wang [2] and Hubert Razik [3]

[1] Logistics Engineering College, Shanghai Maritime University, Shanghai 201306, China
[2] Harbin Institute of Electrical Machinery, Harbin 150040, China
[3] Laboratoire Ampère, Université de Lyon, UMR 5005, F-69007 Lyon, France
* Correspondence: tzwang@shmtu.edu.cn

Abstract: Power extraction has become a critical consideration in tidal stream turbine (TST) systems. In practice, the lumped disturbances under varying tidal current conditions may deteriorate the maximum power point tracking (MPPT) performance and cumulate fatigue damage over-rated power. Besides, the conventional pitch controllers are sensitive to parameter uncertainties of the nonlinear TST system. In this paper, a novel output power internal control strategy based on pseudo-tip-speed ratio and adaptive genetic algorithm (PTSR-AGA) is proposed to improve the anti-interference ability and reliability. The proposed control scheme consists of two parts. The first part proposes the PTSR method for MPPT to predict the TST's operating point which contributes reducing the logical errors assigned to swell disturbances. The second part designed an AGA for the optimization of the pitch controller to conduct its angle delay. A reduced pitch control strategy is applied to the preprocessing of the pitch controller to reduce the mechanical wear over the rated power. The comparative simulation results validate the TST system can obtain a higher power efficiency of energy capture and a smoother power output with the proposed control strategies at full range of tidal current speed.

Keywords: tidal stream turbine; pseudo-tip-speed ratio; pitch control; maximum power point tracking; mechanical wear

Citation: Cai, Y.; Li, M.; Wang, T.; Wang, X.; Razik, H. An Output Power Interval Control Strategy Based on Pseudo-Tip-Speed Ratio and Adaptive Genetic Algorithm for Variable-Pitch Tidal Stream Turbine. *J. Mar. Sci. Eng.* **2022**, *10*, 1197. https://doi.org/10.3390/jmse10091197

Academic Editors: Rafael Morales and Eva Segura

Received: 7 July 2022
Accepted: 20 August 2022
Published: 26 August 2022

1. Introduction

In recent decades, renewable energy resources have attracted extensive attention due to the energy crisis and environmental pollution [1,2]. The tidal current energy is considered as the most promising energy resource due to its regularity, stability, higher energy density, and predictability [3]. However, the tidal stream turbine (TST) system usually operates on complex seabed environments, such as marine organisms, swell effect, and strong storms [4,5]. These factors bring great challenges for the TST system to extract maximum power extraction and estimate the potential marine current energy [6]. To improve the power capture ability of the TST system under the rated flow velocity with these external disturbances, maximum power point tracking (MPPT) strategies are developed to obtain the optimal rotational speed. Moreover, in the event of large spring tides or strong sea states [7], mechanical fatigue of the rated power TST system may appear during the dynamic process. The mechanical wear will shorten turbines' lifetime in the long term, and the maintenance cost of the TST is always too high. Therefore, when the TST system operates above the rated power, the MPPT strategy must be changed into pitch control for smoothing the output power.

In the partial load region of the TST system, the anti-interference ability in revising the power coefficient is significantly expected for the MPPT strategies and tidal energy extraction [8] under swell effect. The tip speed ratio (TSR) and optimum torque (OT)

control MPPT strategies are commonly used in recent [9,10]. However, the TSR strategy requires costly flow equipment, and the OT method relies on the mathematical relationship. In [11], the adaptive perturb and observe (P&O) algorithm is proposed to improve convergence and track efficiency. However, the seabed environmental issues cause frequent changes in flow velocity [12], this method is sensitive to current speed changes and may occur misleading problems. In the full load region, the output power is expected to be kept at a rated value to guarantee system reliability and reduce maintenance costs. The gain-scheduling proportional-integral-derivative (GSPID) pitch control strategy [13] has frequent pitch action due to the tidal current speed disturbances, which increases the risk of sealing damage. In [14], a collective blade-pitch control strategy is proposed to reduce unreliability from the pitch actuator and current sensitivity, while it is difficult to establish the analytical law between the variation of pitch angle and flow velocity for the nonlinear TST system. In [15], feedback linearization theory is applied to solve nonlinear problems. However, it is still greatly affected by variations of uncertain parameters and external disturbances. The classical PID control strategy is more popular in pitch control systems due to its robustness and simplicity of structure [16,17]. While the parameter setting of the PI controller may be a tedious task that requires expert experience, especially when the TST system is dynamic nonlinear and the pitch actuators are subjected to parameter variation. In [18], a variable pitch controller is designed by combining a back-propagation neural network to tune the PI parameters. However, its convergence procedure is unstable, especially under strong external disturbances. In [19], a fuzzy-model predictive controller is designed to adjust the pitch actuator's parameters and reduce the pitch angle error with fine adaptability. However, its coefficients are subject to lumped disturbances and uncertainties. In [20,21], a high-order sliding mode controller (HOSMC) is applied to enhance the robustness of the nonlinear systems with parameter variation. However, the chattering problem of these methods will lead to a stronger power oscillation. In [22], an adaptive single neural controller (ASNC) solves the above problems well, while the time delay of pitch action results in the pitch angle error and increases the PMSG mean load. In [23,24], a fuzzy-model predictive controller is designed to adjust the pitch actuator's parameters to reduce the pitch angle error with fine adaptability. However, its coefficients need to be reset to deal with the disturbances and uncertainties, this method hardly obtains perfect generalization for the nonlinear TST system. In [25], a pitch control strategy based on a particle swarm optimization algorithm demonstrated a good regulation of mismatched parameters. However, the convergence time determined by the range of search space is too long. Such an algorithm is similar to the intelligent optimization methods in [26,27] and has a challenge in capturing the optimal switching time from training to utilization. It is hard to ignore the complexity involved. In [28], a distributed parallel firefly algorithm is applied to PID parameter tuning of variable pitch controller, this strategy can smooth the power output effectively. However, it is easy to fall into the local convergence and optimization failure. In [29,30], the novel intelligent genetic algorithm (GA) is adopted to search for the optimal parameters of the pitch controller, this strategy can enhance the iteration limit by increasing the mutation rate. Simulation results show the control efficiency is 17% greater than that of the classical algorithm. However, the frequent change of pitch angle increases the aerodynamic load on the turbine and has a serious impact on the grid-connected TST system when the current speed fluctuates.

For the problem of lumped disturbances and parameter uncertainties of the nonlinear TST system, a new output power internal control strategy based on pseudo-tip-speed ratio and adaptive genetic algorithms (PTSR-AGA) is proposed to improve the reliability of the TST system in this paper. Firstly, considering the logic misjudgment of the P&O MPPT caused by the swell effect, a PTSR MPPT algorithm is improved to shorten the convergence time for maximum power capture below the rated flow. Secondly, when the current speed exceeds the rated speed, an AGA is designed to mitigate the pitch angle delay caused by uncertain variation in the nonlinear TST system. Thirdly, the power safety margin is also set to reduce the frequent action of the pitch actuator and prolong the lifetime of the sealing

TST system. The effectiveness and feasibility of the proposed control strategy are verified through a simulation model of a 1.5MW TST system with various flow velocities.

The structure of this paper is organized as follows. In Section 2, a detailed description of the TST model and problems of the power interval control scheme are proposed. In Section 3, a PTSR MPPT method is applied to capture the maximum power in the partial load operation, and then a reduced pitch control strategy based on AGA is proposed for power limiting in the full-load operation of the TST system. In Section 4, comparative simulation results verify the superiority of the proposed PTSR-AGA control strategies. Section 5 summarizes this paper and puts forward future research.

2. Problem Description

2.1. Disturbances of Variable Tidal Current Speed under Swell Effect

This paper focuses on a PMSG-based horizontal-axis TST system, which can effectively convert tidal current energy into electrical energy. The mechanical power P_m and torque T_m captured by the TST are as follows [31]:

$$P_m = 0.5\rho\pi R^2 v_{tide}^3 C_p(\lambda, \beta) \tag{1}$$

$$T_m = P_m/\omega_r \tag{2}$$

where ρ is the water density; R is the radius of the tidal wheel; β is the pitch angle of the TST system; ω_r is the rotational speed; C_p is the power coefficient which is described as Equation (3):

$$\begin{cases} C_p(\lambda, \beta) = c_1(c_2/\lambda_i - c_3\beta - c_4)e^{-c_5/\lambda_i} + c_6\lambda \\ 1/\lambda_i = 1/(\lambda + 0.08\beta) - 0.035/\left(\beta^3 + 1\right) \end{cases} \tag{3}$$

Parameters of the PMSG-based TST system prototype are given in Table 1.

Table 1. Parameters of the TST system.

Parameter	Value
Turbine	
Sea water density	1027 kg/m^3
Turbine blade radius	8 m
Rated flow velocity	2.2 m/s
Optimal tip-speed ratio	8.1
Maximum power coefficient	0.48
Rated power	0.8 MW
DC-bus voltage	1500 V
PMSG	
Pole pair number	125
Permanent magnet flux	2.458 Wb
stator resistance	0.0081 Ω
D-axis inductance	1.2 mH
Q-axis inductance	1.2 mH
System inertia	1.3131 × 10^5 Kg·m^2

Based on the analysis of tidal current data and swell characteristics in [7], the tidal current speed v_{tide} can be described in Figure 1.

From Figure 1, tidal currents are strongly disturbed by the swell effect, and the peak tidal speed can reach 3.6 m/s under the spring tides or long-distant storms. Compared with wind speed, the tidal current speed is relatively lower and its range is narrower. According to Equation (3) the frequent fluctuations of water have a higher impact on maximum power point (λ_{opt}, $C_{p\text{-max}}$) tracking in Figure 2a. The power coefficient C_p for each β can reach a maximum value $C_{p\text{-max}}$ at the optimum tip-speed ratio λ_{opt}. Therefore, the maximum power coefficient is achieved when $\beta = 0$. The existing adaptive P&O algorithm [11] is usually adopted for MPPT, as shown in Figure 2b, which is simulated based on Equation (1).

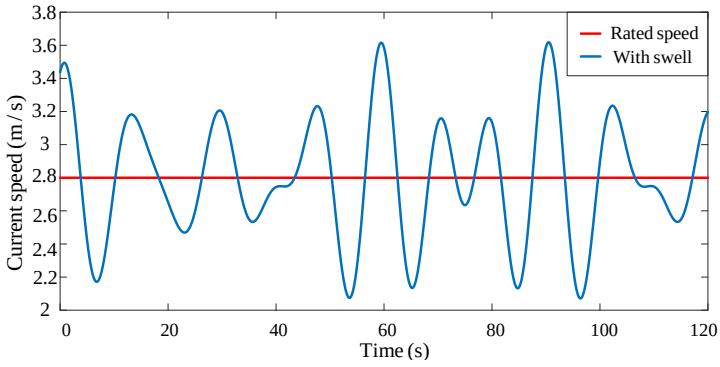

Figure 1. Swell effect on tidal current speed.

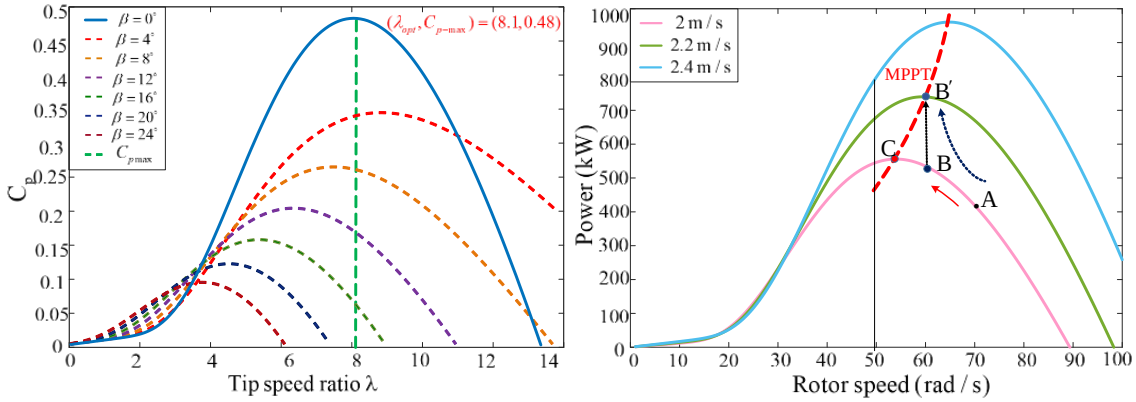

(**a**) (**b**)

Figure 2. (**a**) The TST power coefficient curve; (**b**) Misguided perturbations of the P&O algorithm.

When the current speed rises from 2 m/s to 2.2 m/s in this figure, the maximum power point has been changed from point C to B', the perturbation interval is detailed as:

$$\begin{cases} \omega_{ref}(k) = \omega_r(k-1) + \omega_{step} sign(\Delta P_m / \Delta \omega_r) \\ \omega_{step} = k_{mppt} dP_m / d\omega_r \end{cases} \quad (4)$$

where k_{mppt} is a positive constant. However, with frequently variable tidal current speeds, the actual scenario is $A \rightarrow B'$ instead of $A \rightarrow B$ as expected in Figure 2b due to frequent current speed disturbance. The misguided perturbation ω_{step} in Equation (4) leads to inevitable oscillations near the optimal tip speed radio λ_{opt}:

$$\lambda_{opt} = R\omega_{ref} / v_{tide} \quad (5)$$

Considering spring tides or strong sea states, a conventional pitch control system must provide continuous pitch action to limit the output power by tracking variable tidal current speeds, as described by Equation (6):

$$C_{p\text{-max}}(\lambda_{opt}, \beta) = 2P_{rated} / (\rho \pi R^2 v_{tide}^3) = k_{opt} / v_{tide}^3 \quad (6)$$

where P_{rated} is the limited power of the rated tidal current speed, k_{opt} is the optimum power constant. Pitching frequently in Equation (6) is not reasonable for the TST system, as it accelerates the risk of seal damage and leakage [32].

2.2. Impacts of Parameter Uncertainties and Time-Delay in the Nonlinear TST System

The permanent magnet synchronous generator (PMSG) is usually applied in the TST systems because of its high efficiency and reliability. An $i_d = 0$ field-oriented control method based on PMSG is adopted in this work, where the d–q transformation is replaced with

a commutation scheme that generates the desired current for the desired torque. The dynamic model of PMSG is described in [33] in the synchronous rotation $d-q$ frame as Equation (7):

$$\begin{cases} u_d = R_s i_d + L_d di_d/dt - L_q i_q \omega_r \\ u_q = R_s i_q + L_q di_q/dt + (\psi_f + L_d i_d)\omega_r \\ Jd\omega_r/dt = T_m - T_e - D\omega_r \\ T_e = 3n_p i_q \psi_f/2 \end{cases} \tag{7}$$

where i_d, i_q, L_d, L_q are currents, and inductances; R_s, ψ_f are the generator resistance and magnet flux respectively; J is the TST system total inertia; n_p, D are the pair of poles and friction damping coefficient. u_d, u_q are the d-q axis voltages which can be obtained from the voltage equation in Equation (7). The control strategy can transform the d-q axis voltages into u_α, u_β which are fed to SVPWM algorithm to produce the proper duty cycles for the inverter. Compared with wind turbines, the TSTs installed under complex seabed environments are considered artificial reefs and will be attached by a variety of marine organisms [34], which leads to stronger mass disturbances for the TST blades as Equation (8):

$$\hat{m} = m + m_0 \tag{8}$$

where m_0 is an additional mass of the marine organisms. According to the dynamic changes of blades' masses, the actual TST system total inertia can be described by Equation (9).

$$\hat{J} = \int r^2 d\hat{m} = J + \widetilde{J} \tag{9}$$

where r is the distance from the barycenter of the blades to the hub-center. Considering the variable tidal current speed under significant swell waves and strong sea states, the turbine aerodynamic torque and rotor speed can be expressed as:

$$\hat{T}_m = T_m + \widetilde{T}_m \tag{10}$$

$$\hat{\omega}_r = \int [(\hat{T}_m - T_m)/\hat{J}]d\tau = \omega_r + \widetilde{\omega}_r \tag{11}$$

where $\widetilde{T}_m, \widetilde{\omega}_r$ are the deviation of turbine torque and rotor speed under external disturbances. According to Equations (10) and (11), the mechanical motion equation in the PMSG model can be computed as:

$$\hat{J}d\hat{\omega}_r/dt = \hat{T}_m - T_e - D\hat{\omega}_r + \gamma \tag{12}$$

where γ represents the lumped disturbances of parameter uncertainties. When the TST system operates overload under spring tides or strong sea states, the extracted power of the TST system in Equation (1) must be limited to P_{rated} by pitch controllers to reduce the power coefficient [7], as described in Equation (13):

$$\begin{cases} \hat{\lambda}_{opt} = \hat{\omega}_r R/v_{tide} \\ C_{p\text{-max}}(\hat{\lambda}_{opt}, \beta) = c_1(c_2/\lambda_i - c_3\beta - c_4)e^{-c_5/\lambda_i} + c_6\hat{\lambda}_{opt} \\ 1/\lambda_i = 1/(\hat{\lambda}_{opt} + 0.08\beta) - 0.035/(\beta^3 + 1) \\ \hat{P}_m = 0.5\rho\pi R^2 v_{tide}^3 C_{p\text{-max}}(\hat{\lambda}_{opt}, \beta) = P_m + \widetilde{P}_m \end{cases} \tag{13}$$

where λ_i is the intermediate variable. From Equation (13) and Figure 2, it can be found that a slight deviation of rotor speed leads to a lag delay of the output power $\widetilde{P}_m$. However, the conventional pitch controller relays on the accurate TST system model, which presents parameter uncertainties in harsh working conditions as Equation (12). The actual pitch angle reference can be represented as:

$$\begin{cases} \hat{e} = P_m + \widetilde{P}_m - P_{rated} = e + \widetilde{e} \\ \hat{\beta}_{ref} = k_p(1 + k_i/s)(e + \widetilde{e}) = u_\beta + \delta \end{cases} \tag{14}$$

where u_β is the output pitch angle of the classic pitch controller, k_p, k_i are the proportional and integral coefficients of the pitch controller; δ is the delayed pitch angle, which eventually leads to the deterioration of power control and system dynamic performance. Genetic algorithms (GA) [29,30] represent the ideal tool for robust parameter approximation with easy access to locally optimal solutions. Therefore, the selection of crossover and mutation factors is significant to the adaptive search capabilities for system uncertainty and response speed for pitch controllers.

3. Power Interval Control Scheme for TST System

Figure 3 shows the double-loop power interval control scheme based on PTSR-AGA proposed in this paper. From the power control perspective, there are two operation states of the TST system. The first part is the partial load operation. The pseudo-tip-speed ratio (PTSR) MPPT control strategy is adopted to obtain desired speed ω_{ref} for the generator-side converter controller. This method effectively evades the logic errors attributed to the swell effect and achieves higher maximum power extraction efficiency. In another full load region, considering the mechanical wear and optimal solution of pitch controller, a reduced variation pitch control strategy based on the adaptive genetic algorithm (AGA) is proposed to smooth the power output of the TST system. This provides an appropriate pitch angle for the TST under the lumped disturbances so that the output power of the TST system can be limited and smoothed within a safety margin to protect the unit.

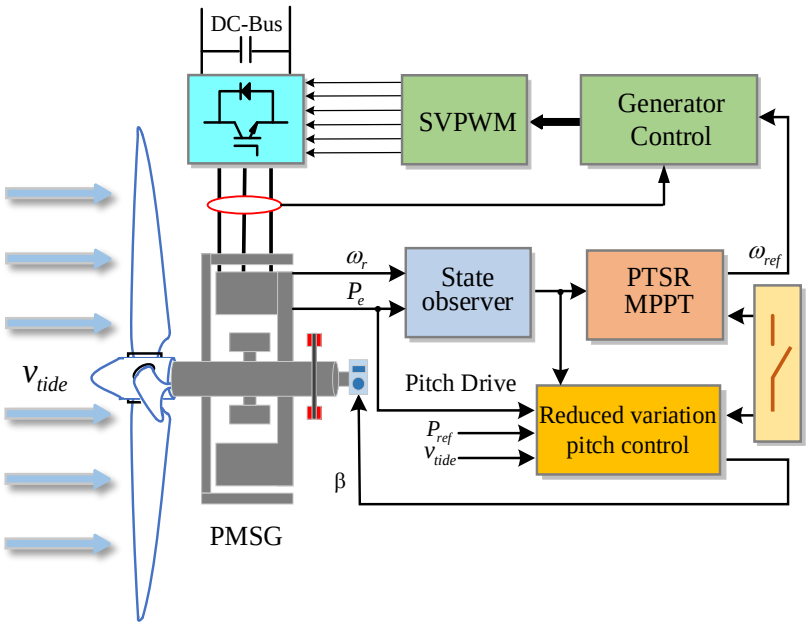

Figure 3. The general control scheme for a direct-driven TST system.

3.1. PTSR MPPT Control for the TST Based on SA Methodology below Rated Flow Velocity

To solve the problem of power oscillation and logical errors in the P&O MPPT with swell fluctuations, a PTSR method is proposed to predict an equivalent rotor speed value based on the slope-assisted (SA) theory to improve the tracking accuracy and stability effectively.

Recalling the curve of $C_{p\text{-max}}$ and the TSR in Figure 2, the output power captured by the TST shown in Equation (1) can be derived as:

$$P_{\max} = 0.5\rho S C_{p\text{-max}} \omega_r^3 R^3 / \lambda_{opt}^3 \tag{15}$$

In case of external disturbances, the adaptive P&O MPPT strategies [11,22] have difficulty controlling the TST system to search for the optimal operating direction accurately

due to frequent current speed changes. Meanwhile, the SA methodology can linearize the output power into the equivalent power P_{SA} with a constant slope value m_λ, designed by:

$$P_{SA} = \sqrt[3]{P_{\max}} = (R/\lambda_{opt})\sqrt[3]{0.5\rho S C_{p\text{-max}}}\omega_r = m_r\omega_r \tag{16}$$

From the determination of m_r in Equation (16), SA methodology considers the slope value m_r as the reference in event of any marine current disturbance, then all optimal operating points are predicted for the TST system with the same aerodynamic characteristics.

Figures 4 and 5 respectively show two different operating statuses of the TST system when detecting the power decreases from point A to B, described as follows:

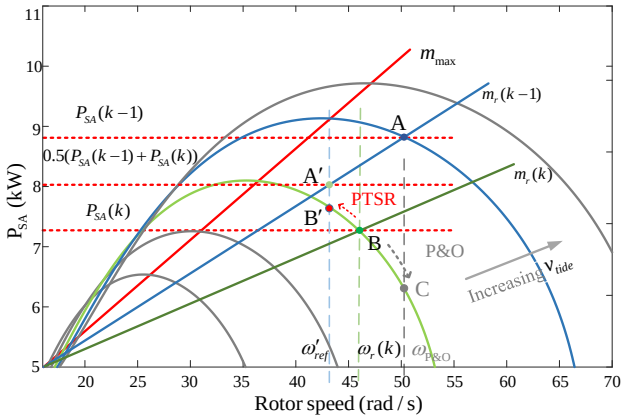

Figure 4. Slope guidance when $m_r(k) < m_r(k-1)$.

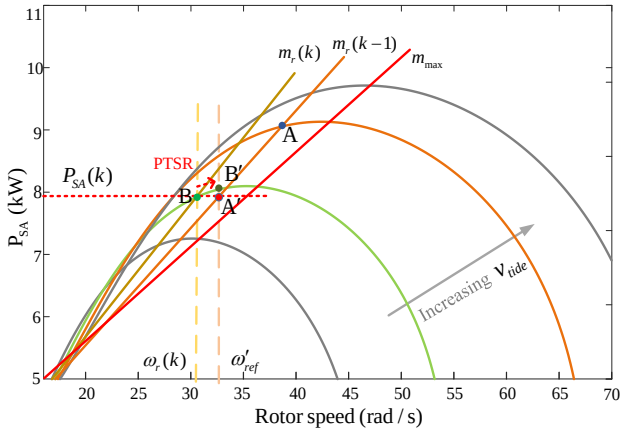

Figure 5. Slope guidance when $m_r(k) > m_r(k-1)$.

Case 1: When $m_r(k) < m_r(k-1)$, as shown in Figure 4, P&O MPPT law only reverses tracking direction to point C which is a logic error. However, the slope values guide back to the previous known TSR state (point B') and determine the best search direction of the MPP by monitoring the power speed change radio (PSCR), as shown in Equation (17).

Case 2: When $m_r(k) > m_r(k-1)$, as shown in Figure 5, the PTSR method uses the pseudo-TSR value to determine the inter-reference in Equation (18), and the best course of the trajectory is from B' to A' with a shorter tracking distance from the MPP.

$$PSCR = abs[(P_{SA}(k) - P_{SA}(k-1))/(\omega_r(k) - \omega_r(k-1))] \tag{17}$$

$$\omega'_{ref} = \begin{cases} 0.5(P_{SA}(k-1) + P_{SA}(k))/m_r(k-1), & m_r(k) < m_r(k-1) \\ P_{SA}(k)/m_r(k-1), & m_r(k) > m_r(k-1) \end{cases} \tag{18}$$

The final output reference of PTSR MPPT is obtained as Equation (19):

$$\omega_{ref}(k) = \omega'_{ref}(k) + PSCR \cdot sign(\omega_{\Delta}) \tag{19}$$

The above analysis shows that the PTSR MPPT strategy can not only evaluate the power fluctuation, but also take the occasional maximum power tracking error into consideration. Therefore, it is robust with respect to frequent tidal current changes.

3.2. Reduced Variation Pitch Control Strategy Based on AGA for the TST Over-Rated Flow Velocity

With the aim to decrease mechanical wear of the pitch sealing mechanism over the rated power, a reduced variation pitch control strategy is proposed to preprocess the pitch controller to improve the pitch control precision and unit protection. While classical pitch controllers are sensitive to the dynamic uncertainties of the TST system, an adaptive fitness law of AGA is proposed for the intelligent optimization of pitch controller's gains K_p, K_i to suppress the effect of pitch angle delay.

3.2.1. Processing of Pitch Controller Based on a Reduced Pitch Variation Method

Considering the unstable seabed environmental conditions, the significant fluctuations in flow velocity force frequent variation in pitch actuators. This solution will accelerate the sealing damage and increase the risk of leakage for the TST system in the long run. Therefore, a reduced pitch variation method is proposed to reduce the pitching frequency of the pitch controller for sealing protection. The pitch variation direction σ is determined according to the power error ratio e_{power} and the trend of current speed variation Δv_{tide}, expressed as follows:

$$e_{power} = (P_m - P_{ref})/P_{ref} \tag{20}$$

$$\sigma(e_{power}, \Delta v_{tide}) = \begin{cases} +1 & , \quad e_{power} > +\varepsilon \ \& \ \Delta v_{tide} > 0 \\ 0 & , \quad |e_{power}| \le \varepsilon \\ -1 & , \quad e_{power} < -\varepsilon \ \& \ \Delta v_{tide} < 0 \end{cases} \tag{21}$$

where P_{ref} is the rated power value of the TST system. Figure 6 shows the pre-processed pitch control diagram. The pitch actuator does not act within the preset safety power allowance of $[-\varepsilon, +\varepsilon]$ defined at ±5% of the rated power [14]. When the output power of the TST system is beyond this range, the input error of the pitch controller will increase accordingly and can be calculated as in Equation (22):

$$e_{input} = \sigma(e_{power}, \Delta v_{tide}) \sqrt{(e_{power} - \varepsilon)^2 + \Delta v^2_{tide}} \tag{22}$$

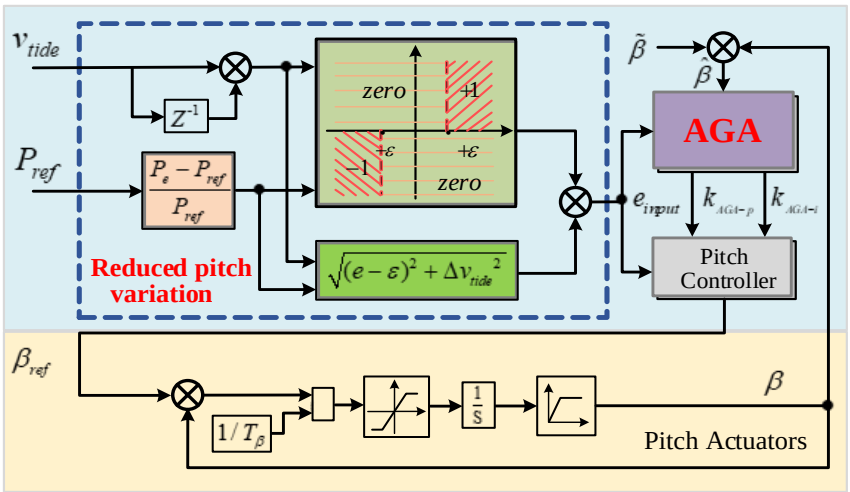

Figure 6. Diagram of reduced variation pitch control based on AGA.

3.2.2. Optimization of Pitch Controller Based on AGA

Compared with standard GA [29,30,35,36], two improvements of the proposed AGA to solve the pitch angle delay problem mentioned in Section 2 are stated as follows:

- Correction of delayed pitch action based on fitness law of AGA
- Based on the blade element theory [13], the effect of pitch angle delay on classical pitch controllers is presented in Figure 7. The actual pitch angle can be expressed as:

$$\hat{\beta} = \beta + \widetilde{\beta} \tag{23}$$

where $\widetilde{\beta}$ is the pitch angle deviation, w is the relative velocity of tidal current to the plane of rotation; ∂ is the angle of the attack, which is fixed as rated value. The delayed pitch angle $\beta(k - T_{\beta-delay})$ output from the pitch controller leads to the imprecise adjustment to current speed variation Δv_{tide}. To solve the pitch angle delay under different sea conditions, the actual pitch angle is considered in the cost function H, designed as:

$$H = \gamma \int |e_{input}| + (1-\gamma) \int \hat{\beta}^2 \tag{24}$$

$$F = A/(H + 10^{-6}) \tag{25}$$

where γ is the coefficient used to compromise error and pitch action, and A is a positive constant value.

- External disturbance suppression based on dynamic crossover and mutation operator

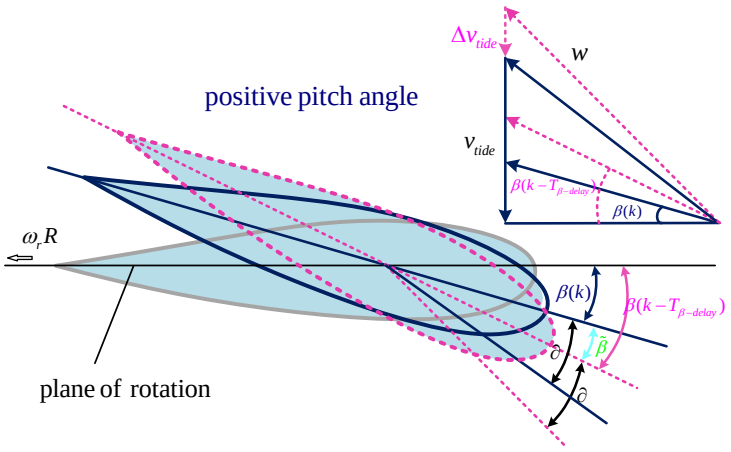

Figure 7. Schematic of blade pitch action delay caused by parameter uncertainty of the TST system.

Due to the lumped disturbances under the spring tides or strong storms, the standard GA can easily access locally optimal solutions, which hampers the global searching performance and system reliability. In this paper, a flexible AGA adopts an adaptive mechanism to select the crossover and mutation probability, detailed as follows:

$$p_c = \sqrt{G+1}/c_0 \tag{26}$$

$$p_m(i) = |0.1 - 2i/N|(p_{\max} - p_{\min}) \tag{27}$$

where G is the number of generations, N is the total population size, and c_0 is the constant coefficient. $p_{\max}$, $p_{\min}$ are respectively the maximum and minimum mutation probability sorted by fitness size. The crossover factor in Equation (26) can be adjusted online according to the number of iterations to reduce the adjustment error of the pitch angle. The mutation probability in Equation (27) is designed as the fitness function of each individual.

$$\begin{cases} F_1(e_{input}, \hat{\beta}) > \ldots > F_i(e_{input}, \hat{\beta}) > \ldots > F_N(e_{input}, \hat{\beta}) \\ p_{\min} < p_m(1) < \ldots < p_m(i) < \ldots < p_m(N) < p_{\max} \end{cases} \tag{28}$$

As shown in Equation (28), for the individuals with greater fitness, the lower mutation probability is employed in the new populations to shorten the response speed of the pitch control strategy.

The output of the pitch controller with AGA optimization is:

$$\beta_{ref}(k) = \beta_{ref}(k-1) + k_{AGA-p}[e_{input}(k) - e_{input}(k-1)] + k_{AGA-i}e_{input}(k) \quad (29)$$

The dynamic behavior of the pitch actuator in Figure 6 can be described as Equation (30). The final pitch angle of the TST system is obtained by Laplace transform, as shown in Equation (31):

$$\dot{\beta} = (\beta_{ref} - \beta)/T_\beta \quad (30)$$

$$\beta = \beta_{ref}/(T_\beta s + 1) \quad (31)$$

where β_{ref} is the optimal pitch angle output from the proposed reduced variation AGA-PI controller, T_β is the pitch action time constant. To reduce the risk of pitch actuator damage from overuse, the pitch angle is limited to a range of $[-2°, 30°]$ in normal operation. Figure 8 shows a flowchart of the AGA optimization method used to tune pitch controller parameters online for the TST system. The process in the red dotted box presents the details of step 3 AGA.

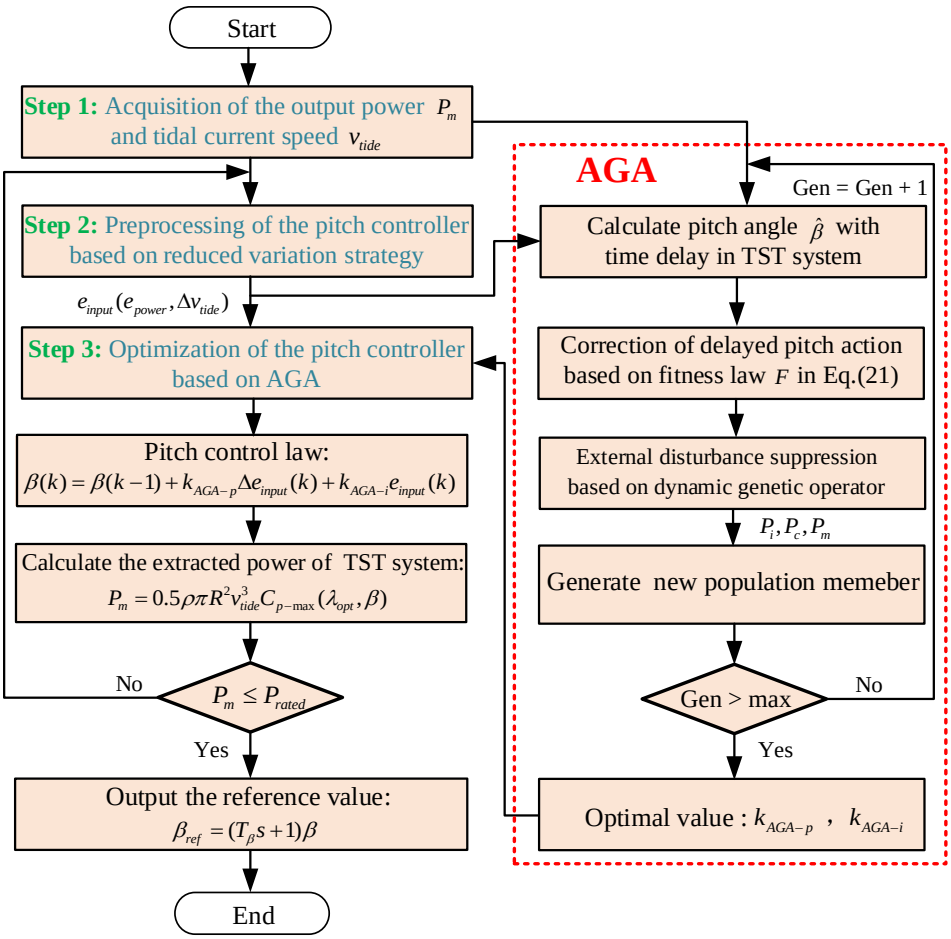

Figure 8. Detailed flowchart of the proposed adaptive genetic algorithm (AGA).

The specific control steps of Figure 8 are as follows:

(1) The controller receives P_m, V_{tide} from the TST. According to the optimized preprocessing Equation (22), the input error value e_{input} of the pitch controller is obtained and input to the proposed AGA.

(2) The AGA calculate pitch angle $\hat{\beta}$ with time delay. According to the actual range of the PI parameters to be optimized, the AGA generates an initial population and set the number of iterations Gen.
(3) Different from the traditional genetic algorithm, AGA uses Equation (25) as the fitness function.
(4) Genetic operation: According to the fitness function and the principle of survival of the fittest, the individual with the highest fitness value and the greatest adaptability to the parameter uncertainty of the pitch control system is selected. Then, the crossover probability and mutation probability are adjusted according to the adaptive rate determined by Equations (26) and (27) to perform crossover and mutation calculation to generate a new population.
(5) Optimization termination: Once the number of iterations reaches the maximum value Gen, the optimal value k_{AGA-p}, k_{AGA-i} is obtained by a comparison of fitness function and sent to the pitch controller. If $P_m \leq P_{rated}$, the controller outputs the reference pitch angle value.

4. Simulation Results and Analysis

To verify the effectiveness of the proposed PTSR-AGA for the variable-pitch TST system, the platform based on a direct-drive PMSG based TST system prototype is used as the basis for numerical simulation in Matlab2016b. Comparative simulations with GSPID, HOSMC, ASNC, and P&O-GA are carried out with a 1.5 MW TST system, and the characteristics of them are shown in Table 2. The platform is successfully tested by EDF (French Electricity) off the coast of Paimpol-Bréhat (France). The specific parameters of the TST system [37] are listed in Table 1. In this paper, the relevant parameters of the PTSR-AGA are considered: $\varepsilon = 0.05$, $N = 40$, $G = 200$, $A = 14$, $c_0 = 17.7$, and the range of mutation probability is $p_m = [0.01, 0.1]$ for the AGA.

Table 2. The characteristics of various control strategies.

Strategy	Characteristics
GSPID	Simple structure and easy parameter tuning, but low response or saturation;
HOSMC	High robustness of the nonlinear system with parameter variation, but chatting problem and power oscillation;
ASNC	Great adaptability and anti-interference, but increased mean load;
P&O-GA	Enhanced the iteration limit by increasing the mutation rate; but frequent pitch action.

Considering the complexity and variability of the seabed environment, the real-tidal flow velocity in Figure 1 shows highly turbulent fluctuation in the range of ± 0.4 m/s, and even the high-tidal velocity rises to the peak of 3.6 m/s during 12–18 s, 27–33 s, and 46–50 s. While tidal current speeds exceed the rated value of 2.8 m/s, the conventional GS-PID pitch control strategy outputs the highest angle of 5.3°, and its pitch action has a delay of 2 s, as illustrated in Figure 9a. The HOSMC method reduces the pitch action greatly with a delay of 0.8 s, and the ASNC and P&O-GA show smaller amplitudes of the pitch angle. In contrast, the maximum pitch angle of the proposed PTSR-AGA method is less than 0.4° within the acceptable range, and the response speed is much faster than the above control strategies.

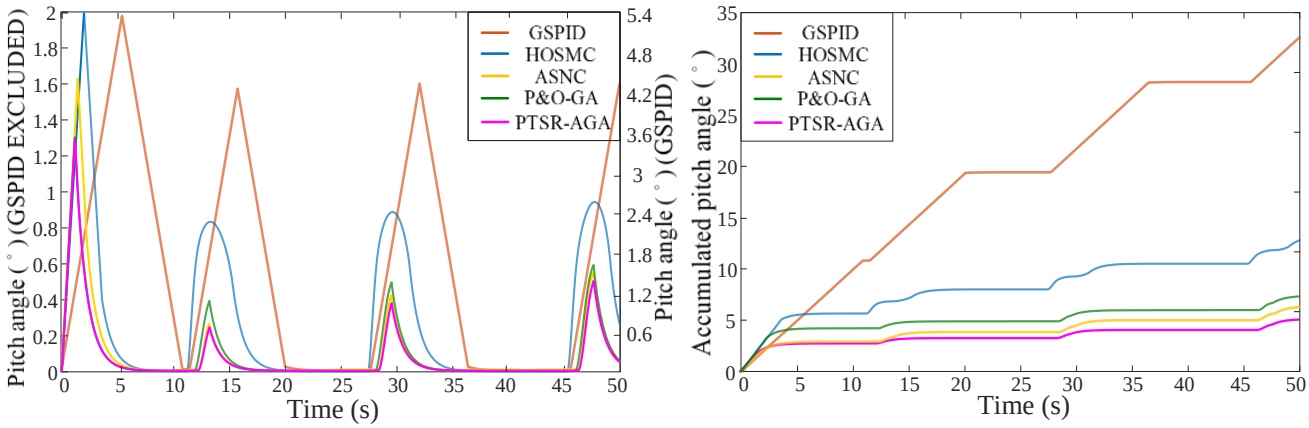

Figure 9. (**a**) Comparative results of pitch angle; (**b**) Accumulated angle of comparative methods.

To quantify the total pitch action, the accumulated pitch angle of comparative methods is introduced in Equation (32):

$$\beta_a = \sum_{i=1}^{n} |\beta(i) - \beta(i-1)| \tag{32}$$

As shown in Figure 9b, the accumulated pitch angle of the HOSMC is decreased to 11.102° compared to 32.433° of the conventional control strategy. The ASNC and P&O-GA display lower pitch angle moment variations, while the proposed pitch control strategy has only 4.28° with the best power-limiting performance over the rated current speed.

Blow the rated power, the variable current speed of the TST system fluctuates frequently under external disturbances. To validate the robustness and stability of the PTSR-AGA control strategy, the power coefficient and rotational speed tracking performance of five comparative control strategies are shown in Figure 10a,b. The HOSMC can accurately identify the TST system's maximum power point with negligible oscillations compared to the conventional method when a lower current speed is detected. While the ASNC and P&O-GA methods show stronger anti-interference ability with the tracking error of 0.03 rad/s. However, compared with the average search time of the P&O-GA strategy (10.1742 s), the proposed PTSR-AGA has a shorter average search time of 8.7805 s. This obtains a higher average C_p value and the smallest MPPT error of 0.005 rad/s compared to other methods.

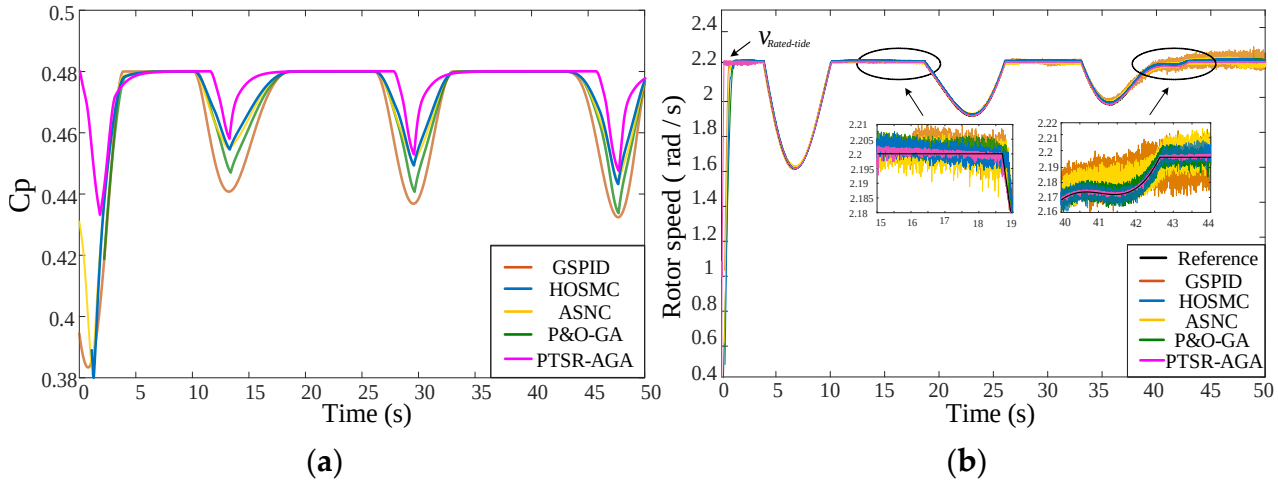

Figure 10. (**a**) Comparison of power coefficients; (**b**) Rotor speed tracking of the proposed method.

To have a better comparison of the five control strategies, the following three performance indices, IAE (integral absolute error) [22], FAP (fractional average power), and IAPE (integral absolute power error) [38], in Table 3, are considered:

$$\begin{cases} IAE = \int |e(t)|dt \\ FAP = \sum_{i=1}^{n} (P_t(i)/P_{tide}(i))/n = \sum_{i=1}^{n} C_p(i) \\ IAPE = \int |P(t) - P_{rated}|dt \end{cases} \quad (33)$$

where *IAE* represents the overall performance of speed tracking response, the *FAP* emphasizes the power capture performance during the low current speed periods, the fewer *IAPE* means better power limiting performance and regulation. Figure 11a shows the output power curves of five control strategies under different sea conditions. The conventional GSPID method is greatly affected by external disturbances and has an undesirable *IAPE* value of 2.01×10^4 kW. Although the HOSMC can suppress the chatting and improve the power extraction efficiency, this method shows negligible pitch angle variations of 11.102°. Considering the large inertia and parameter uncertainties of the TST system, the ASNC and P&O-GA strategies confine the power within the safety allowance range with lower IAPE of 1.64×10^4 kW and 1.56×10^4 kW. However, the power fluctuation is still large with a maximum amplitude of 0.41×10^2 kW and an overshoot of 5.125%. While the proposed PTSR-AGA method outputs smoother power of only 1.01×10^4 kW with the highest *FAP* index of 23.4 under the premise of efficient energy generations. From the perspective of total energy generated by the TST system, as shown in Figure 11b, the conventional GA-PID strategy obtains nearly 7.64 kWh, while the ASNC and P&O-GA methods capture more energy with 15.03 kWh and 15.51 kWh better than the HOSMC by 11.2% and 14.78% respectively. However, the proposed PTSR-AGA yields the maximum energy with 15.55 kWh, so the system guarantees the higher-energy capture efficiency under both turbulent and strong sea storm conditions.

Table 3. The performance indexes of five control strategies.

	IAE	FAP	IAPE (kW)	β_a	Energy (kWh)
GSPID [38]	1.74	20.5	2.01×10^4	32.433°	7.64
HOSMC [21]	1.65	22.8	1.42×10^4	11.102°	13.52
ASNC [22]	1.68	23.3	1.64×10^4	4.94°	15.51
P&O-GA [29]	1.62	23.1	1.56×10^4	5.076°	15.03
PTSR-AGA	0.328	23.4	1.01×10^4	4.28°	15.55

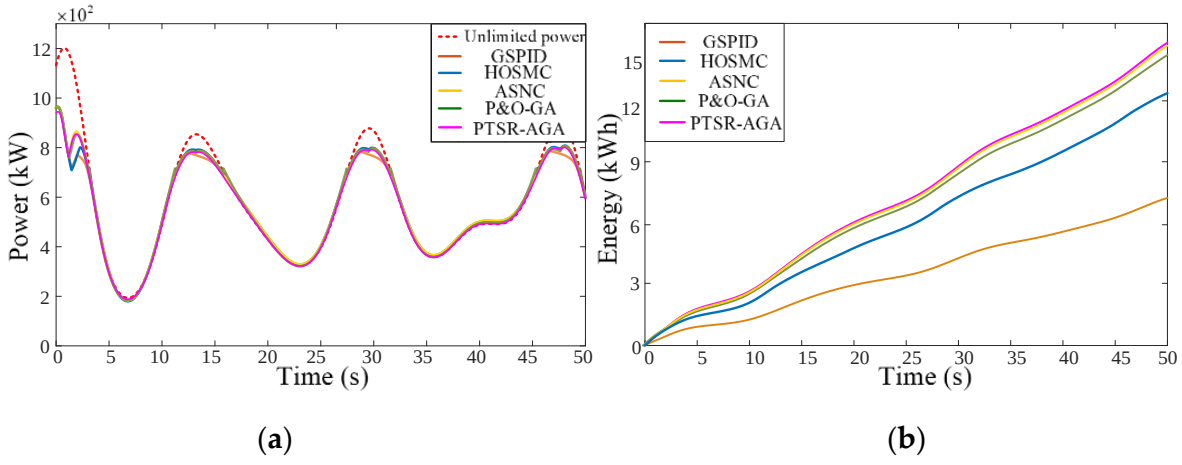

(**a**) (**b**)

Figure 11. (**a**) Comparison of active power; (**b**) Generator Energy of the comparative methods.

5. Conclusions

An output power interval control strategy based on PTSR-AGA is proposed in this paper to mitigate the output power oscillation under lumped disturbances and reduce mechanical wear of the TST system. Firstly, a PTSR MPPT strategy is proposed to minimize the logic error of P&O MPPT under swell effect with a shorter convergence time, which improves the power capture efficiency of the TST system at low flow velocity. Secondly, the influence of parameter uncertainties in the nonlinear TST system is analyzed during over-rated current speed, which can cause time delay in the optimization of the pitch controller. An adaptive fitness law is designed for the AGA to mitigate pitch angle delay and improve the real-time performance and precision. Subsequently, a reduced variation pitch control strategy is proposed to depress the mechanical wear of the TST, so the output of smoother power contributes to protecting the unit and prolonging the lifetime of the TST system. Finally, the effectiveness and feasibility of the PTSR-AGA method are verified under different sea conditions through numerical simulations. The achieved results demonstrate that the proposed control strategy not only effectively reduces pitch action and leak damage caused by mechanical wear, but also improves the disturbance suppression ability of the TST system.

Author Contributions: Conceptualization, Y.C., M.L. and T.W.; methodology, Y.C., M.L. and T.W.; software, M.L.; formal analysis, Y.C. and M.L.; writing—original draft preparation, Y.C., M.L. and T.W.; writing—review and editing, Y.C., M.L., T.W., X.W. and H.R. All authors have read and agreed to the published version of the manuscript.

Funding: This research was funded by National Natural Science Foundation of China and Natural Science Foundation of Shanghai, China, grant number 62073213 and 16ZR1414300.

Institutional Review Board Statement: Not applicable.

Informed Consent Statement: Not applicable.

Data Availability Statement: All data in this study has been included in this paper.

Conflicts of Interest: The authors declare no conflict of interest. The funders had no role in the design of the study; in the collection, analyses, or interpretation of data; in the writing of the manuscript; or in the decision to publish the results.

References

1. Hao, C.; Tang, T.; Ait-Ahmed, N.; Benbouzid, M.; Zaim, E.H. Attraction, challenge and current status of marine current energy. *IEEE Access* **2018**, *6*, 665–685.
2. Guillou, N.; Charpentier, J.-F.; Benbouzid, M. The Tidal Stream Energy Resource of the Fromveur Strait—A Review. *J. Mar. Sci. Eng.* **2020**, *8*, 1037. [CrossRef]
3. Panda, K.P.; Anand, A.; Bana, P.R.; Panda, G. Novel PWM Control with Modified PSO-MPPT Algorithm for Reduced Switch MLI Based Standalone PV System. *Int. J. Emerg. Electr. Power Syst.* **2018**, *19*, 287–293. [CrossRef]
4. Djebarri, S.; Charpentier, J.F.; Scuiller, F.; Benbouzid, M. Design methodology of permanent magnet generators for fixed-pitch tidal turbines with overspeed power limitation strategy. *J. Ocean. Eng. Sci.* **2020**, *5*, 73–83. [CrossRef]
5. Tao, X.A.; Tw, A.; Qh, B.; Dda, C.; Cca, D. A review of current issues of marine current turbine blade fault detection. *Ocean. Eng.* **2020**, *218*, 16.
6. Xie, T.; Wang, T.; Diallo, D.; Razik, H. Imbalance Fault Detection Based on the Integrated Analysis Strategy for Marine Current Turbines under Variable Current Speed. *Entropy* **2020**, *22*, 1069. [CrossRef] [PubMed]
7. Zhou, Z.; Scuiller, F.; Charpentier, J.F.; Benbouzid, M.E.H.; Tang, T. Power control of a nonpitchable PMSG-based marine current turbine at overrated current speed with flux-weakening strategy. *IEEE J. Ocean. Eng.* **2015**, *40*, 536–545. [CrossRef]
8. Blunden, L.S.; Bahaj, A.S. Tidal energy resource assessment for tidal stream generators. *Proc. Inst. Mech. Eng. Part A J. Power Energy* **2007**, *221*, 137–146. [CrossRef]
9. Saidi, Y.; Mezouar, A.; Miloud, Y.; Brahmi, B.; Benmahdjoub, M.A. Adaptive maximum power control based on optimum torque method for wind turbine by using fuzzy-logic adaption mechanisms during partial load operation. *Period. Polytech. Electr. Eng. Comput. Sci.* **2020**, *64*, 15155. [CrossRef]
10. Dao, N.D.; Lee, D.C.; Lee, S. A simple and robust sensorless control based on stator current vector for PMSG wind power systems. *IEEE Access* **2019**, *7*, 8070–8080. [CrossRef]

11. Ahmed, J.; Salam, Z. A modified P&O maximum power point tracking method with reduced steady-state oscillation and improved tracking efficiency. *IEEE Trans. Sustain. Energy* **2016**, *7*, 1506–1515.
12. Bryden, I.G.; Couch, S.J.; Owen, A.; Melville, G. Tidal current resource assessment. *Proc. Inst. Mech. Eng. Part A J. Power Energy* **2007**, *221*, 125–135. [CrossRef]
13. Gu, Y.J.; Liu, H.W.; Li, W.; Lin, Y.G.; Li, Y.J. Integrated design and implementation of 120-kW horizontal-axis tidal current energy conversion system. *Ocean. Eng.* **2018**, *158*, 338–349. [CrossRef]
14. Gu, Y.J.; Lin, Y.G.; Xu, Q.K.; Liu, H.W.; Li, W. Blade-pitch system for tidal current turbines with reduced variation pitch control strategy based on tidal current velocity preview. *Renew. Energy* **2018**, *115*, 147–158. [CrossRef]
15. Nguyen, A.T.; Lee, D.C. Advanced LVRT strategy for SCIG-based wind energy conversion systems using feedback linearization and sliding mode control. *J. Power Electron.* **2021**, *21*, 1180–1189. [CrossRef]
16. Li, P.; Hu, W.; Hu, R.; Chen, Z. The primary frequency control method of tidal turbine based on pitch control. *Energy Procedia* **2018**, *145*, 199–204. [CrossRef]
17. Youcef, B.; Abdelyazid, A.; Farid, H.; Mendil, B.; Ullah, N. Robust energy-based nonlinear observer and voltage control for grid-connected permanent magnet synchronous generator in tidal energy conversion system. *Int. J. Energy Res.* **2021**, *45*, 13250–13268.
18. Ren, H.; Hou, B.; Zhou, G.; Shen, L.; Li, Q. Variable pitch active disturbance rejection control of wind turbines based on BP neural network PID. *IEEE Access* **2020**, *8*, 71782–71797. [CrossRef]
19. Bustan, D.; Moodi, H. Adaptive interval type-2 fuzzy controller for variable-speed wind turbine. *J. Mod. Power Syst. Clean Energy* **2020**, *10*, 524–530. [CrossRef]
20. Hao, C.A.; Qi, L.A.; St, A.; Aa, B.; Jh, A.; Tw, A. Adaptive super-twisting control of doubly salient permanent magnet generator for tidal stream turbine. *Int. J. Electr. Power Energy Syst.* **2021**, *128*, 106772.
21. Wang, X.F.; He, L. FPGA-Based Predictive Speed Control for PMSM System Using Integral Sliding-Mode Disturbance Observer. *IEEE Trans. Ind. Electron* **2021**, *68*, 972–981. [CrossRef]
22. Li, M.-Z.; Wang, T.Z.; Zhou, F.N.; Shi, M. An adaptive single neural control for variable step-size P&O MPPT of marine current turbine system. *China Ocean. Eng.* **2021**, *35*, 750–758.
23. Abdelbaky, M.A.; Liu, X.; Jiang, D. Design and implementation of partial offline fuzzy model-predictive pitch controller for large-scale wind-turbines. *Renew. Energy* **2020**, *145*, 981–996. [CrossRef]
24. Ren, H.; Zhang, H.; Deng, G. Feedforward feedback pitch control for wind turbine based on feedback linearization with sliding mode and fuzzy PID algorithm. *Math. Probl. Eng.* **2018**, *2018*, 4606780. [CrossRef]
25. Smida, M.B.; Sakly, A. Smoothing wind power fluctuations by particle swarm optimization-based pitch angle controller. *Trans. Inst. Meas. Control.* **2019**, *41*, 647–656. [CrossRef]
26. Hu, P.; Pan, J.S.; Chu, S.C. Improved binary grey wolf optimizer and its application for feature selection. *Knowl. Based Syst.* **2020**, *195*, 105746. [CrossRef]
27. Deng, W.; Xu, J. An enhanced MSIQDE algorithm with novel multiple strategies for global optimization problems. *IEEE Trans. Syst. Man Cybern. Syst.* **2020**, *52*, 99. [CrossRef]
28. Shan, J.; Pan, J.S.; Chang, C.K.; Chu, S.C.; Zheng, S.G. A distributed parallel firefly algorithm with communication strategies and its application for the control of variable pitch wind turbine. *ISA Trans.* **2021**, *115*, 79–94. [CrossRef]
29. Hicham, C.; Mehdy, K.; Okezie, O.; Hamid, G. Simplified speed control of permanent magnet Synchronous Motors Using Genetic Algorithms. *IEEE Trans. Power Electron.* **2019**, *34*, 3563–3574.
30. Liu, Z.; Liu, X.; Wang, K.; Liang, Z.; Correia, J.A.; De Jesus, A.M. GA-BP neural network-based strain prediction in full-scale static testing of wind turbine blades. *Energies* **2019**, *12*, 1026. [CrossRef]
31. Zhou, X.; Wang, T.; Diallo, D. An active disturbance rejection sensorless control strategy based on sliding mode observer for marine current turbine. *ISA Trans.* **2020**, *124*, 403–410. [CrossRef] [PubMed]
32. Ahmed, U.; Apsley, D.D.; Afgan, I.; Stallard, T.; Stansby, P.K. Fluctuating loads on a tidal turbine due to velocity shear and turbulence: Comparison of cfd with field data. *Renew. Energy* **2017**, *112*, 235–246. [CrossRef]
33. Li, S.; Cao, M.; Li, J.; Cao, J.; Lin, Z. Sensorless-based active disturbance rejection control for a wind energy conversion system with permanent magnet synchronous generator. *IEEE Access* **2019**, *7*, 122663–122674. [CrossRef]
34. Li, Z.; Wang, T.; Wang, Y.; Amirat, Y.; Diallo, D. A wavelet threshold denoising-based imbalance fault detection method for marine current turbines. *IEEE Access* **2020**, *8*, 29815–29825. [CrossRef]
35. Castro, A.; Guazzelli, P.; Oliveira, C.; Pereira, W.; Monteiro, J. Optimized current waveform for torque ripple mitigation and MTPA operation of PMSM with back EMF harmonics based on genetic algorithm and artificial neural network. *IEEE Lat. Am. Trans.* **2020**, *18*, 1646–1655. [CrossRef]
36. Rezaei, N.; Uddin, M.N.; Amin, I.K.; Othman, M.L.; Marsadek, M. Genetic Algorithm based optimization of overcurrent relay coordination for improved protection of DFIG operated wind farms. *IEEE Trans. Ind. Appl.* **2019**, *55*, 5727–5736. [CrossRef]
37. Zhou, Z.; Scuiller, F.; Charpentier, J.F.; Benbouzid, M.E.H.; Tang, T. Power smoothing control in a grid-connected marine current turbine system for compensating swell effect. *IEEE Trans. Sustain. Energy* **2013**, *4*, 816–826. [CrossRef]
38. Amirhossein, A.; Reza, S.; Ali, J. Performance and robustness of optimal fractional fuzzy PID controllers for pitch control of a wind turbine using chaotic optimization algorithms. *ISA Trans.* **2018**, *79*, 27–44.